RADIATION DRIVEN WINDS OF HOT STARS – SOME REMARKS ON STATIONARY MODELS AND SPECTRUM SYNTHESIS IN TIME-DEPENDENT SIMULATIONS

Joachim Puls[1], *Adalbert W.A. Pauldrach*[1], *Rolf-Peter Kudritzki*[1,2], *Stanley P. Owocki*[3], *Francisco Najarro*[1]

[1] Institut für Astronomie und Astrophysik der Universität München, Scheinerstrasse 1, D–W–8000 München 80, Germany.

[2] Max-Planck-Institut für Astrophysik, Karl-Schwarzschild-Strasse 1, D–W–8046 Garching, Germany.

[3] Bartol Research Institute, The University of Delaware, Newark, DE 19716, USA.

1 Introduction

Although few in number, hot massive stars are important constituents of the stellar population, both in terms of their enormous luminosity and their mass loss. Because of their prodigious radiation field, they are ideal standard candles visible at large distances, either directly or indirectly by ionizing HII-regions. By their supersonically expanding winds and the corresponding mass loss, they contribute significantly to the chemical evolution of galaxies as continuous sources of nuclear processed material and provide a considerable fraction of interstellar dust (Wolf-Rayet stars in their late phases). The energy and momentum of the wind controls the energy balance of the surrounding interstellar matter and may induce the formation of new stars.

In addition, without understanding the origin and dependence of stellar mass loss on stellar parameters, the complete evolution in the upper HRD is an open question, since different evolutionary scenarios are a consequence of the assumed (or derived) mass loss in the different stages of evolution (O/Of stars, luminous blue variables (LBV's), Wolf-Rayet stars (WR's) , central stars of planetary nebulae (CSPN)).

Finally, it became evident during the last few years that the determination of stellar parameters from the analysis of photospheric lines by means of hydrostatic NLTE model atmospheres, which were so far considered as the most reliable tools to obtain effective temperatures, gravities and abundances, is severely affected by the emission of surrounding winds, at least in cases when the mean wind density is high (cf. Abbott and Hummer, 1985; Gabler et al., 1989; Voels et al., 1989; Kudritzki, 1992; Becker and Butler, 1992; Sellmaier et al., 1993). Hence, even the comparison of a theoretical and "observed" HRD for evolved or extremely massive stars is prohibitive if the diagnostics do not account for the presence and strength of the stellar wind.

It is therefore extremely important to develop a consistent theory which enables us to derive the wind parameters and structure from first principles, i.e. as function

of stellar parameters (L, M, R, metallicity), and to investigate the predicted spectral appearance of those models by a *detailed comparison with observations at all wavelengths.*

Over the last two decades, it has generally been established that the most favorable driving mechanism for the winds from hot, luminous OB stars is the line scattering of the stellar UV radiation field by heavy ions in the expanding stellar wind. Building upon the pioneering work by Lucy and Solomon (1970), Castor, Abbott and Klein (1975; hereafter CAK) and Abbott (1980, 1982a), current models now solve self-consistently the time-independent hydrodynamics (Pauldrach, Puls, Kudritzki, 1986; see also Friend and Abbott, 1986) together with the NLTE equations of state for all contributing ions (Pauldrach, 1987) and the radiative transfer allowing for multiple scattering (Puls, 1987). Such models are able to reproduce quantitatively numerous observed stationary features for a variety of hot stars of different metallicity (Kudritzki et al., 1987) and evolutionary status (O/Of stars: Pauldrach et al., 1990; CSPN: Pauldrach et al., 1988; P Cygni (LBV): Pauldrach and Puls, 1990). Among these are:

- the terminal velocity and time-averaged mass loss rate;
- the complete far UV spectrum including P-Cygni profiles from subordinate lines and, in many cases, even from "superionized" species;
- the "SiIV luminosity effect" (cf. Walborn and Panek, 1985);
- the optical and IR H/He lines and the observed IR and thermal radio excess (cf. Gabler et al. 1989).

(For a recent review and references, see Kudritzki et al., 1991).

In §2.1, we will briefly discuss the basic concept of these stationary models and show, as an example for the present application, the way in which these models are used for and in how far they influence the determination of stellar and wind parameters of massive hot stars(§2.2)

However, as follows directly from the assumption of stationarity, these models are inherently incapable of describing a number of additional observational features, which immediately show that the nonstationary aspects of the wind must be of significant importance. A number of these features will be discussed in §3.1, but listed briefly, they include:

- the soft X-ray emission (Harnden et al., 1979, Seward et al. 1979);
- the discrete absorption components (DAC's) often observed in the absorption parts of unsaturated lines (Lamers et al., 1982; Prinja and Howarth, 1986; Henrichs, 1988 and references therein);
- the temporal variability of the wind lines, where the blue edges are varying most significantly, while the red emission part remains relatively constant (e.g. Henrichs, 1991 and Prinja, 1991);
- the electron-scattering wings of recombination lines in Wolf-Rayet stars, which are weaker than models predict, suggesting the possibility of a clumped structure (Hillier, 1991);

- the black troughs in saturated P-Cygni profiles (Lucy, 1982, 1983), which in the present stationary description are simulated by a velocity-dependent turbulence (cf. Hamann, 1981; Puls, 1987; Groenewegen et al., 1989);

- the variability of optical lines such as H_α (Ebbetts, 1982) and HeII 4686 (Henrichs, 1991);

- the nonthermal radio emission observed from roughly 30% of massive stars (cf. Abbott, Bieging and Churchwell, 1981, 1984).

Together these observational properties suggest that these winds have a significant degree of spatial structure and temporal variability. Theoretical efforts to understand the nature and origin of this structure have generally focused on the line-driving mechanism itself, which linear stability analyses have shown to be highly unstable (MacGregor et al, 1979; Carlberg, 1980; Abbott, 1980 ; Lucy 1984; Owocki and Rybicki, 1984, 1985). Subsequent efforts have been concentrated on dynamical modelling of the time-dependent wind structure from direct, numerical simulation of the nonlinear evolution of the line-driven flow instability (for references and recent reviews see Castor, 1991 and Owocki, 1992).

The basic picture resulting from the present dynamical models is discussed in §3.2 and shows the following: Only a very small fraction of material is accelerated to high-speed and then shocked; for most of the matter the major effect is a compression into narrow, dense "clumps" (shells in these 1-D models), separated by large regions of much lower density.

Although the *spatial* variation of the velocity and density seems to be in stark contrast to the stationary picture, the *mass* distribution of these quantities are not so very different (Owocki, Castor and Rybicki (OCR), 1988; Owocki 1990, 1992), and, furthermore, the gross wind properties like the *terminal* flow speed and *time-averaged* mass loss rate turn out to be in quite good agreement with those derived in steady models.

Given the intrinsic mass-weighting of spectral formation, and the extensive temporal and spatial averaging involved, it thus seems quite possible that, in some average sense, the observational signatures of such structured models may actually be quite similar to what's derived from the stationary approach. In this way such models offer the possibility of retaining the very great successes of these stationary models in matching time-averaged observational properties, while also reproducing the many signatures suggesting the existence of extensive wind structure.

It is thus clear that a major effort is needed in the synthesis of observational signatures from these structured models. The complexity of this structure leads to many difficulties not encountered in the smooth stationary case, and we have to develop the corresponding methods in order to allow for an appropriate analysis. This should give us finally the constraints on the actual structure by comparing synthetic spectra and observations. For this purpose, we will present here some first results and implications of recent calculations (cf. Owocki, 1992, Puls and Owocki, 1993) on the synthesis of UV-resonance lines (§3.3.1) and the formation of H_α and the IR- continuum (§3.3.2; Puls, Najarro and Owocki, in prep. for *Astron. Astrophys.*).

General Assumptions

Throughout the present paper, we will use the following assumptions:

- *radiative line driving*: the winds of hot stars are *initiated* and *accelerated* by radiative line driving of UV metal lines where this mechanism was first shown to work actually by Lucy and Solomon (1970) and CAK (1975).
- *time dependence*: in §2, we consider the winds to be stationary, i.e.$\partial/\partial t \equiv 0$, whereas in §3 the time dependence is explicitly taken into account.
- *spherical symmetry* is assumed, as there is no indication of a *significant* polarization in *typical* OB stars. (Be and WR-stars are here not considered).
- in the hydrodynamical description, the mass flow is treated in terms of a *one-component medium*, as the momentum transfer between the driven ions and the bulk of the matter (protons, He-ions) via Coulomb collisions is under most conditions very effective. (cf. Castor, Abbott and Klein, 1976). However, as shown by Springmann and Pauldrach (1992), in thin winds (e.g. winds of main-sequence O-Stars) a decoupling of ions and protons with subsequent ion runaway may be possible before the theoretical v_∞ (assuming a one-component medium) is reached.

2 Stationary Models

2.1 Basic Concept

In order to obtain the hydrodynamical stratification for the *stationary* outflow, the continuity equation (with constant mass-loss $\dot{M}$!) and the equation of motion have to be solved simultaneously. Here, the contributing external forces are the gravity and the radiation force both from continuum (electron-scattering, bound-free-, free-free-processes) and lines, where the latter is the dominating part in the supersonic regime of the wind. The principle process responsible for the line-acceleration can be easily described:

Due to the Doppler-shift in the expanding medium, the absorbing line profile is shifted in frequency with respect to the continuum, so that at each radius *unprocessed* continuum photons are "fed" into the line. To a first approximation, the majority of these photons originate from the stellar photosphere, and so the absorption process is rather anisotropic, covering only the finite cone angle subtended by the stellar disk. On the other hand, the reemission process (spontaneous decay or collisionally induced) is isotropic in the frame comoving with the ion, which leads to a diffuse radiation field with a rough fore-aft symmetry. This means that the force associated with the reemission process is nearly zero, so that in total only *radial* momentum is transferred to the ion. (For a very instructive discussion of this process, cf. Owocki, 1990, 1992). Finally, since a very large number of metal lines can contribute at or near the flux-maximum of a large luminosity ($L_{Bol} \sim 10^4 - 10^6 L_\odot$), the total line-acceleration can overcome the gravity by large factors.

However, the line force depends on the actual capability of absorbing photons - i.e. on the line strengths and hence on the occupation numbers - and on the actual distribution (in frequency and angle) of those photons -i.e. on the radiative transfer;

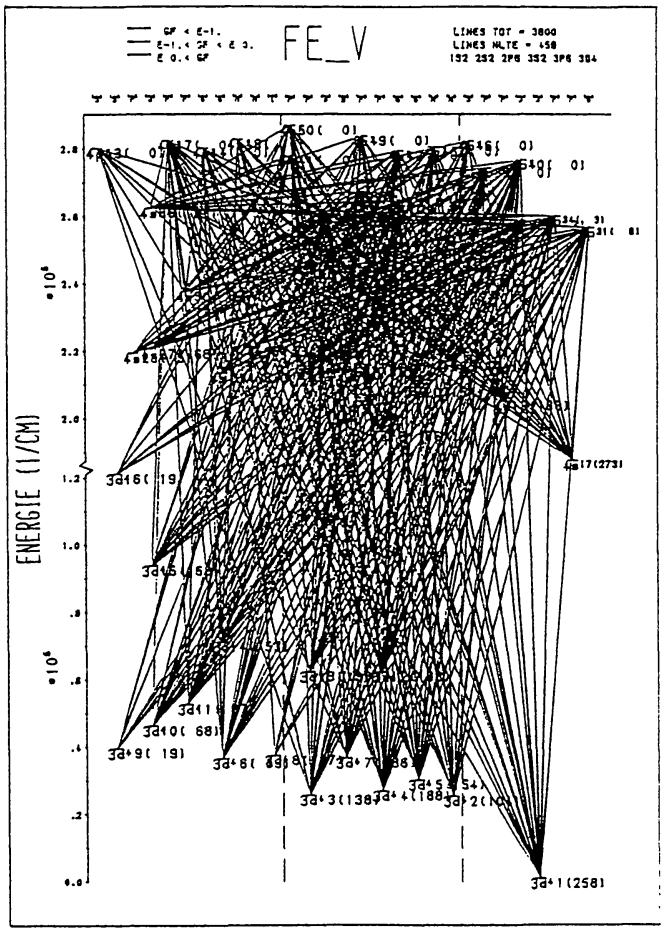

Figure 1: Grotrian diagram for the used FeV ion (data from K. Butler, p.c.).

we thus have to solve for these quantities through a distinct *NLTE*-treatment of *all contributing* ions/levels, since the properties of hot star atmospheres are dominated by the high energy density of the radiation field. In other words, simply the fact that we are considering radiation driven winds with its requirement of the presence of large radiation fields inevitably implies NLTE-conditions.

The question is now: What does *"all contributing"* mean in the present context? Here we have to consider all the ions/levels which are both

–essential for the line driving and
–neccessary in order to establish a correct ionization/excitation equilibrium.

From an inspection of abundances and the ionization/excitation potentials, for the present case a number of

– 26 elements
– 150 ions
– 5,000 levels
– 20,000 connecting line transitions giving rise to a
– NLTE-line force from more than 300,000 lines

have to be taken into account in order to meet these requirements.

The reason that this enormous number of levels/lines can be actually treated in NLTE is based on two factors. First, the *stationary* hydrodynamics is relatively simple and costs, in comparison to the NLTE calculations, little additional computational time. Second, the line-transfer required for each transition is simplified by the presence of the *large* velocity gradient. This enables one to use the so-called Sobolev-approximation (Sobolev, 1957; Castor, 1970), at least if this method is applied in a more general way than in the original formulation by allowing for the effects of an overlapping continuum (Hummer and Rybicki, 1985; Puls and Hummer, 1988) and overlapping lines (Olson, 1982; Puls, 1987).

Nevertheless, from the numbers above it is obvious that a vast amount of atomic data has to be both calculated and accumulated. In addition, effective methods of book-keeping have to be implemented in the numerical codes in order to keep the calculations manageable.

The first effort with respect to the problem of calculating and accumulating the required data was performed by Kurucz and Peytremann (1975), followed by the compilation of those data which are necessary for the specific problem of hot star winds by Abbott (1982).

Meanwhile, however, the results of the "Opacity Project" (Seaton, 1987) are available, and additional data (most important in the present context being Fe) are being calculated by K. Butler and other members of the Munich NLTE group by means of the "superstructure" code (Eissner et al., 1974; Nussbaumer and Storey, 1978). From those calculations, all required information is available with a high degree of precision. As an example for a typical dataset, Fig.1 shows the Grotrian diagram of FeV as used in our calculation. The reader may note that this ion is an important species for hot stars, both in terms of its contribution to the line force (roughly 50 % in the lower wind part) and as a diagnostic tool for inferring abundances (cf. Fig.2 and §2.2).

The first self-consistent models of radiatively driven winds, i.e.models which solve for the hydrodynamics, NLTE-equations and radiative transfer in parallel, were presented by Pauldrach (1987) and Puls (1987). Meanwhile, a number of improvements/additional physics have been added to the original treatment, which is still partly under way. These modifications are summarized and discussed by Pauldrach et al. (1993), where especially the following points are considered:

- the improved atomic physics (esp. for Fe, see above) results in a larger number of contributing lines, which in the end yields a larger $\dot{M}$ in comparison to the old models.

- the influence and importance of the photospheric/wind *line-blocking* on the ionization structure is extensively discussed (cf. also Pauldrach et al., 1990). In the present approach, this process is accounted for only in an approximate way, but the correct treatment (cf. Puls and Pauldrach, 1990) is now being implemented.

- in order to account for the presence of the observed X-rays (cf §3.1) which most probably are emitted in the cooling zones of hot regions heated by shocks propagating throughout the wind, the corresponding radiation field has to be considered. Most important here is the influence of the strong EUV-part of this radiation field on the ionization structure.

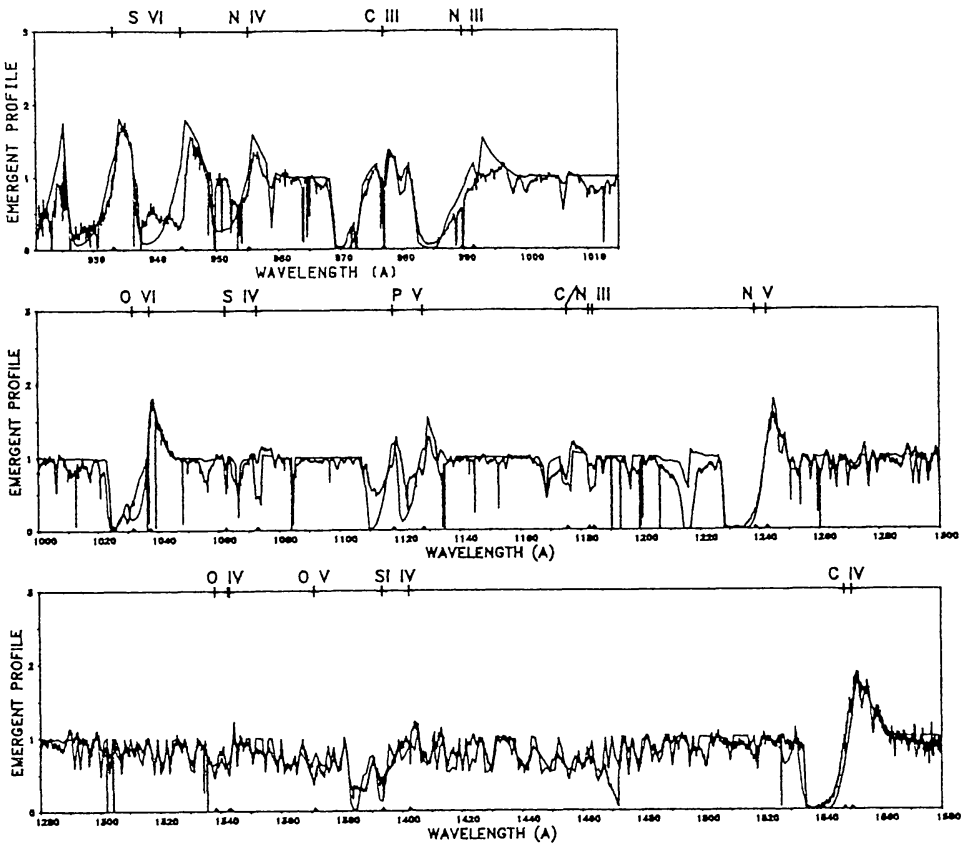

Figure 2: Comparison of Copernicus/IUE observations of ζPup with our present calculations. Note the large number of lines between 1400 and 1500 Å, due mainly to FeV. (From Pauldrach et al., 1993).

As an example of the present state of the art, we show in Fig.2 the theoretical UV-spectrum of ζ *Pup* (O4If) in comparison to observations. The reader may note that our model reproduces the so-called "super-ionization", i.e.the presence of high ionization stages (CIV, NV, OVI) in parallel with low ionization stages (CIII, NIII) in a *cool* wind model ($T_e \lesssim T_{eff}$, from radiative equilibrium), as well as the large number of "photospheric" (but wind-contaminated!) Fe-lines present in the observations.

2.2 Some results – Determination of Stellar and Wind Parameters for O-Stars

(For this section, cf. also the review by Kudritzki et al., 1991)

2.2.1 T_{eff} and $\log g$

The effective temperature T_{eff}, the gravitational acceleration $\log g$ and the Helium abundance of hot stars follow usually from the analysis of photospheric H/He-lines such as H_γ, HeII (4200, 4542) and HeI 4471 (cf. the review by Kudritzki and Hummer, 1990 and Herrero et al., 1992) by means of *hydrostatic, plane-parallel* NLTE atmospheres. However, attention has to be paid to stars that exhibit *strong*

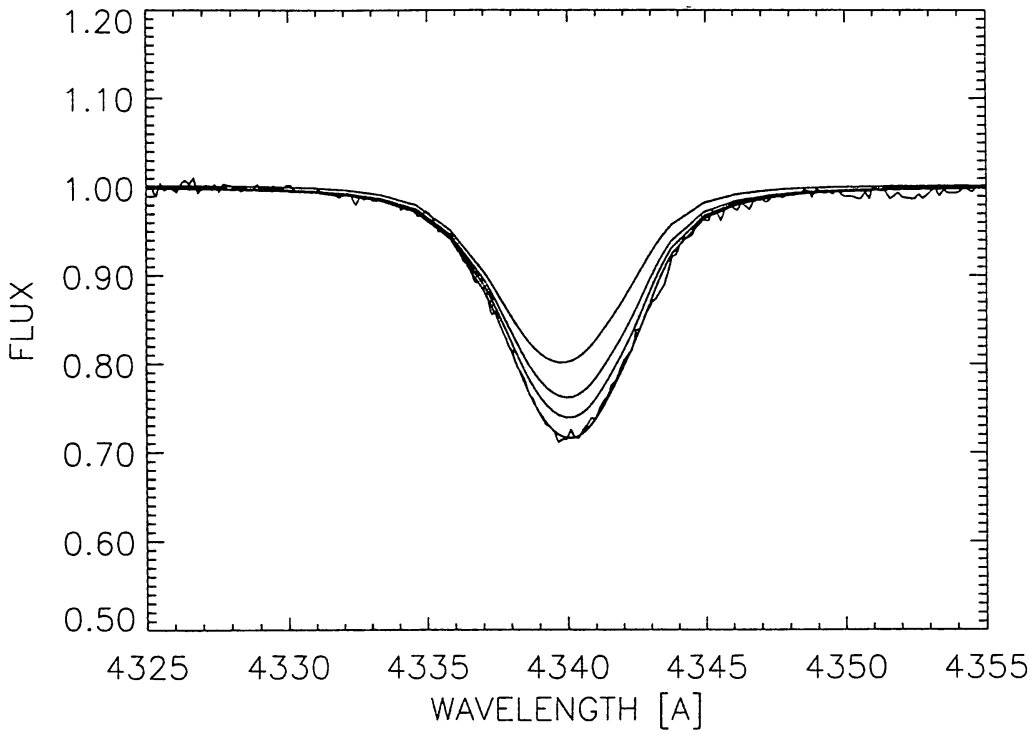

Figure 3: Theoretical profile of H_γ for different $\dot{M}$'s (from 10^{-6} to $10^{-5} M_\odot/yr$) in comparison to observations of ζPup. Adopted stellar parameters are from *hydrostatic, plane-parallel* NLTE-analysis. (From Sellmaier et al., 1993.)

winds, as here these lines can be significantly contaminated by wind effects (cf. Gabler et al.,1989, Sellmaier et al., 1993).

As an example, we show in Fig. 3 the theoretical profile of H_γ – the strategic line to derive $\log g$– for the "unified atmosphere" (cf. Gabler et al., 1989) of ζPup, where the stellar parameters were obtained by the above method (cf. Kudritzki et al., 1983). Inconsistently, however, different $\dot{M}$'s (from 10^{-6} to $10^{-5} M_\odot/yr$) were used in order to simulate the effect of different wind strengths. The observed profile here coincides with the lowest $\dot{M}$ which shows that in thin winds the profile remains uncontaminated. For increasing $\dot{M}$, however, the line is substantially filled with wind emission. As the actual $\dot{M}$ of ζPup is of the order of $3 - 5 \cdot 10^{-6} M_\odot/yr$) (from H_α and thermal radio emission, see below), the difference of the theoretical profile for this $\dot{M}$ and the observation simply illustrates that the adopted stellar parameters (in this case $\log g$) are incorrect and a consistent determination in the "unified" framework has to be performed.

2.2.2 The Terminal Velocity v_∞

The present standard procedure to measure terminal velocities of stellar winds is to use the so-called "SEI" method (cf. Hamann, 1981; Lamers et al., 1987; Groenewegen et al., 1989; Pauldrach et al., 1993) by fitting synthetic profiles of UV-(resonance-)lines (e.g. CIV, NV) to observations and thereby obtain (in addition to other information like the product of $\dot{M}$ times ionization fraction times abundance) the terminal velocity. In order to match the observed profile shape (esp. the

so-called "black trough" and the extendend, gradual blue edge, cf. §3.1), however, one has to adopt a *supersonic* turbulent velocity $v_{turb}(r) \sim 0.1v(r)$. This v_{turb}then broadens the resonance-zones and leads to these desired features (cf. Fig. 5).

A more recent interpretation (Prinja, Barlow, and Howarth, 1990) is to associate the terminal velocity with the maximum velocity of discrete absorption components or with the blue edge of the black trough.

Hence, one should note that the determination of the stationary wind parameter v_∞ requires the use of a turbulent velocity parameter which is a priori inconsistent with the stationary picture.

2.2.3 Mass-Loss Rate $\dot{M}$

The most reliable method to infer $\dot{M}$ is from the radio excess (cf. Wright and Barlow, 1975; Panagia and Felli, 1975; Lamers and Waters, 1984), which depends crucially on the density in the outer part of the wind and hence on $\dot{M}$. The use of this method requires, however, that the emission is thermal (roughly 30% are non-thermal emitters, cf. §1), that the flux is observable (i.e. only for objects in the Galaxy) and that the wind is not clumped or that we know the radial distribution of the clumping in the outer part of the wind. (cf. §3.3.2)

An alternative method to determine $\dot{M}$ is the use of H_α or HeII 4686 as mass-loss indicators, which for obvious reasons is a "must" for extragalactic objects. Although a number of approximate methods exist which determine the equivalent width of H_α as function of $\dot{M}$ (cf. Leitherer, 1988; Drew, 1990; Scuderi et al., 1992), a more accurate analysis requires a NLTE line formation in the complete atmosphere to allow for the influence of departures from LTE, the influence of the Stark wings in the transsonic region and the contamination by the HeII blend (cf. Gabler A. et al., 1990).

2.2.4 Mass, Radius and Distance

(cf. Pauldrach and Puls, 1990a; Kudritzki et al, 1992)

Case 1: Distance known. When the distance is known (e.g. by cluster membership), we can determine both the so-called *"spectroscopic mass"* from log $g$and the distance, and the so-called *"wind mass"* from wind theory

$$v_\infty = f(L, M, T_{eff})$$

which in combination with the spectroscopic T_{eff}, the terminal velocity v_∞ and the stellar luminosity (accounting for the error in distance) results in M. In general, both methods agree well, however the second method has the advantage in that the error bars are significantly smaller (see Kudritzki et al., 1992 and Herrero et al., 1992 (esp. Fig. 15) for many examples of this technique).

On the other hand, if we compare the spectroscopic mass with the *"evolutionary mass"* following from evolutionary calculations (e.g. Maeder, 1990), we find for almost all objects analyzed a significant deviation, with the evolutionary mass being typically larger (cf. Groenewegen et al., 1989, and Herrero et al., 1992, Fig. 14). This problem, which even exists for main-sequence objects, is refered to as the so-called *"mass-problem"* and is one of the major topics in the present discussion of stellar evolution. As pointed out by N. Langer in a recent talk in Munich, possible solutions

may be connected with homogeneous evolution caused by mass-loss, rotationally induced mixing and semi-convection.

Case 2: Distance unknown. If the distance is unknown, we nevertheless can obtain the stellar mass from wind theory since we have an additional relation for $\dot{M}$:

$$v_\infty = f_1(T_{eff}, \log g, R)$$
$$\dot{M} = f_2(T_{eff}, \log g, R)$$

Thus we can derive the surface gravity *and* the radius in parallel from T_{eff}, v_∞ and the observational quantity related to $\dot{M}$

$$\log Q = \log \dot{M} - 3/2 \log(R/R_\odot) \quad \text{from radio, } H_\alpha \text{ or HeII 4686}$$
$$\log D = \log \dot{M} - \log(R/R_\odot) \quad \text{from UV line fits}$$

(Again, for a number of examples, see Kudritzki et al., 1992.) Note that this offers the additional possibility of comparison with spectroscopically derived surface gravities. The stellar *distance* also follows from this method, with a typical precision in the distance modulus $\sim \pm 0.5^m$. Hence, the application of method 2 allows one to determine the radius and distance of *luminous* stars in distant galaxies (local group and beyond!) by using a combination of optical observations ($\rightarrow T_{eff}$, in near future with the ESO-VLT) and UV observations ($\rightarrow v_\infty$, HST).

2.2.5 Analysis of the Atmosphere of the LMC-Star Sk - 66 100

As an example of the application of the method described above, we will show in this section the complete analysis of atmosphere Sk - 66 100 (O6 III, $m_V = 13.3^m$) in the LMC. This analysis is part of a current project involving the HST, where first results are given in Kudritzki et al., 1993. (This paper also presents analysis of Sk-68 137 (O3III) and a re-analysis of Mk42 (O3f/WN).) The objective of this project is the investigation of hot star physics (with particular emphasis on evolution and mass-loss) as function of metallicity. To this end, appropriate samples of massive stars in our galaxy and the MC's have been selected, where the ground based optical programme (ESO 3.6m, CASPEC) is substantially complete. However, following the GHRS failure, the programme had to be reconfigured for FOS/high resolution and hence is somewhat delayed.

Step 1. By detailed fits of the optical lines (observations with ESO 3.6m) with hydrostatic plane-parallel NLTE-atmospheres, the following parameters are derived (cf. Kudritzki et al.,1993, Fig. 5):

$$T_{eff} = 42,000K, \qquad \log g = 3.7, \qquad N_{He}/N_H = 0.1$$

Step 2. From H_α, we find by NLTE line-formation on *unified* atmospheres (cf. Fig. 4):

$$\dot{M} \approx 1.5 \cdot 10^{-6}\ M_\odot/yr$$

Step 3. From Ly_α (UV spectrum by HST/FOS, wavelength coverage from 1150 to 1800 Å), the Hydrogen column density towards the star (both the contribution of the Galaxy and of the LMC) results in

$$\log N_H^{\rm Gal} = 20.4, \qquad \log N_H^{\rm LMC} = 20.55$$

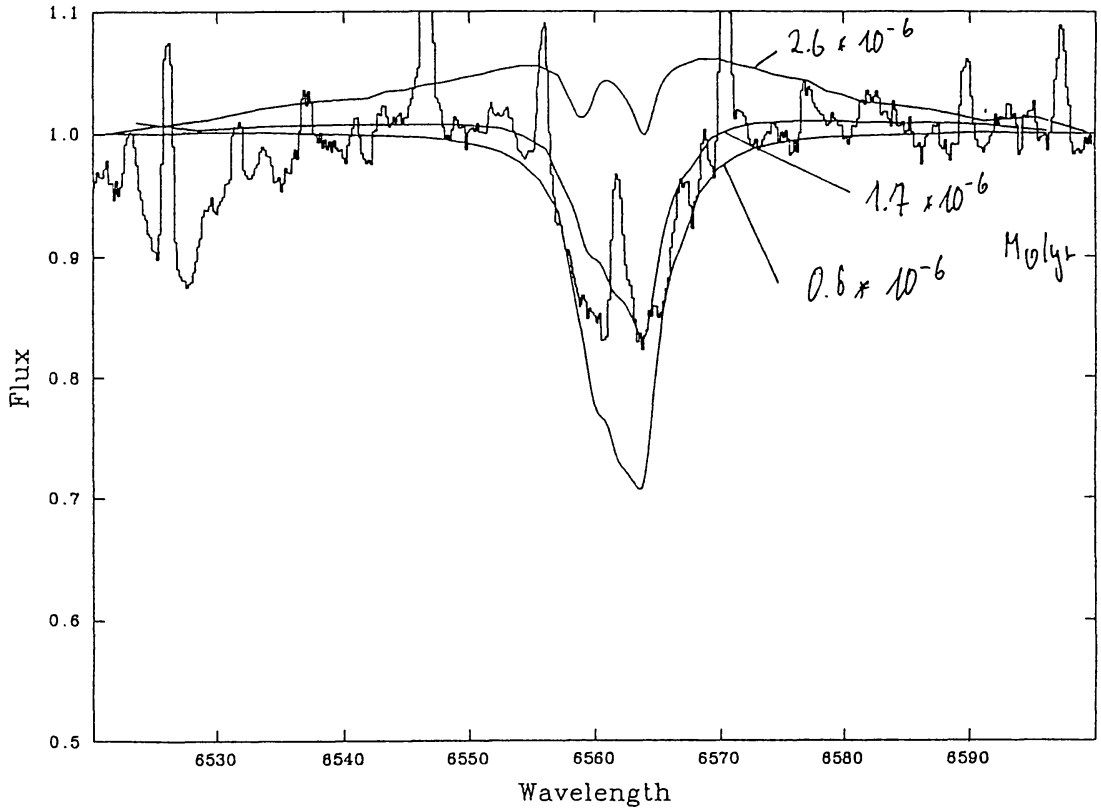

Figure 4: Theoretical H_α profiles based on *unified* atmospheres in comparison to observations of Sk-66 100. (From R. Gabler, p.c.)

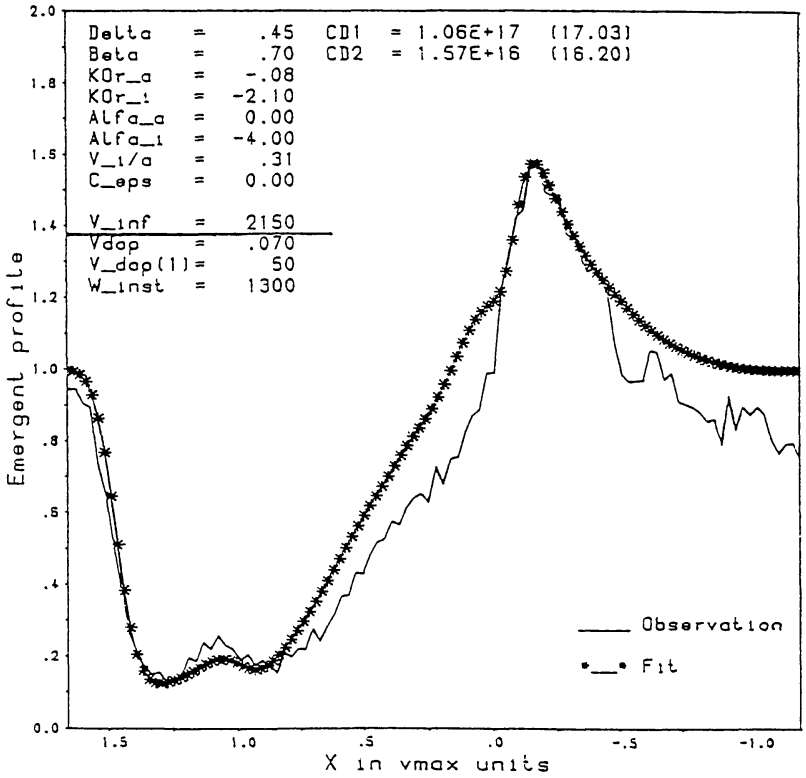

Figure 5: SEI-fit to the NV doublet of Sk-66 100. Observations by HST/FOS. (From S. Haser, p.c.)

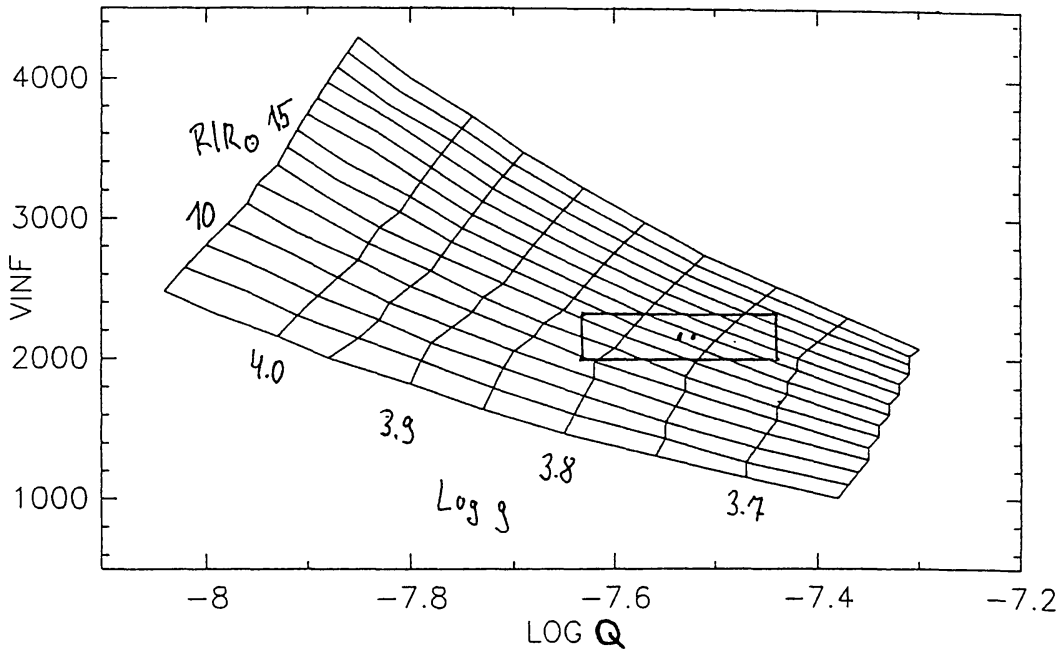

Figure 6: Theoretical fit diagram for Sk-66 100 to determine R_* and $\log g$ from v_∞ and $\log Q$ (cf. §2.2.4 and Kudritzki et al., 1993).

Step 4. The terminal velocity follows from an SEI-fit to the NV-doublet (cf. Fig. 5), as well as the "turbulent velocity".

$$v_\infty = 2,150 km/s, \qquad v_{turb}^{max} = 150 km/s$$

Step 5. With the help of the theoretical fit diagram (T_{eff}= 42,000K) and from v_∞ and $\dot{M}$ we obtain (cf. Fig. 6)

$$R/R_\odot = 14.5\ (+4.5/-3.5), \qquad \log g = 3.77, \qquad m - M = 18.6 \pm 0.6$$

resulting in a wind-mass of $M/M_\odot = 44 \pm 11$.

Step 6. Finally, by simulating different metallicities in our wind code and comparing to the complete UV-spectrum (cf. Fig. 7), the metallicity is roughly

$$Z \approx 1/2\ Z_\odot$$

Note, that we do not claim this as a "standard value" for *the* LMC-abundance; In contrast, the analysis of the other two objects (see above) leads to a more typical value of a quarter solar metallicity.

Hence, by a successive application of the methods introduced above and the use of optical and UV observations, all parameters are determined.

2.3 Conclusion of Section 2

At present, the *stationary* models of radiatively driven winds are able to explain all *gross* observational features of O-star winds, and the phase of application to astrophysical problems related to stellar mass-loss is just in progress. Note, however,

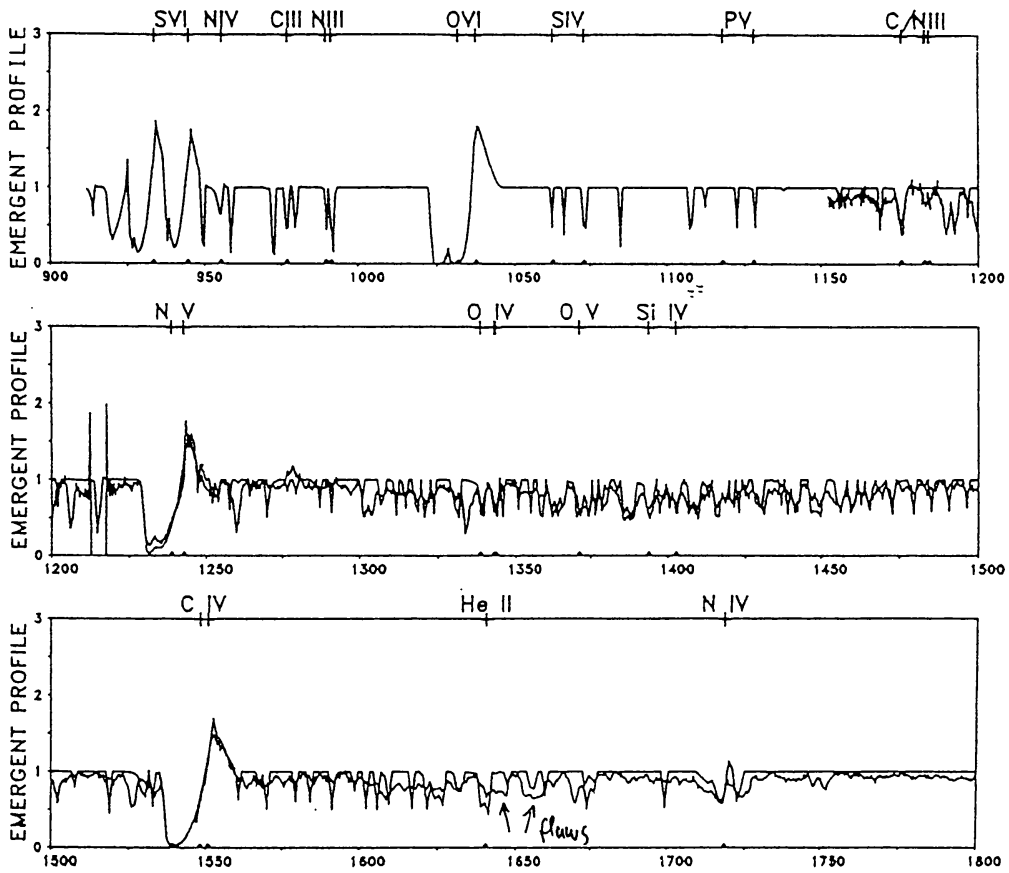

Figure 7: Comparison of the model wind spectrum (half solar metallicity) with the HST/FOS spectrum of Sk-66 100. (From Kudritzki et al., 1993.)

that a detailed analysis requires the incorporation of features characteristic of *non-stationary* processes (e.g. supersonic turbulence and the "hot" EUV and X-ray radiation field created in shocks).

In addition, as pointed out in §1, there exist several other kinds of observational evidence that indicate a significant degree of spatial structure and temporal variability in these winds. Although this may not fit in the stationary picture, the facts cannot be simply pushed away by hand-waving arguments, but have to be carefully considered.

3 Spectrum Synthesis in Time-Dependent Models

3.1 Observational Evidence for Non-Stationary Processes in Stellar Winds

In this section, we will discuss some of the items summarized in §1 that indicate the presence of non-stationary processes.

X-ray emission. Following the detection of the "superionization-" features in O-star winds, it was argued that the presence of the high ionization species (cf. Fig. 2) arise from Auger ionization from X-rays which were at that time however only *postulated* (Cassinelli and Olson, 1979). Although this problem could be partly solved by means of detailed NLTE-calculations (Pauldrach, 1987), the predicted

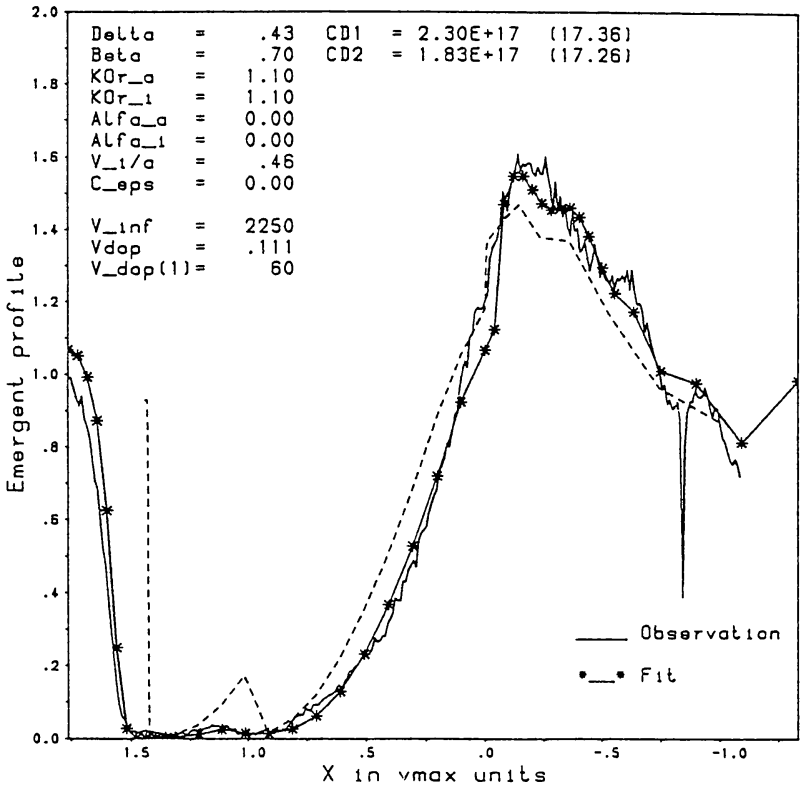

Figure 8: SEI-fit to the NV doublet of ζPup using $v_{turb}^{max} \approx 250 km/s$. The dashed line shows the profile resulting from the same parameters, however with $v_{turb} \equiv 0$. (From S. Haser, p.c.)

X-ray emission was actually observed by the *Einstein* Observatory. A subsequent analysis showed that this emission roughly scales with the stellar luminosity as $L_x \approx 10^{-7}\, L_{Bol}$ (e.g. Long and White, 1980; Chlebowski et al., 1989 and references therein), and the spectra typically show both a soft ($\sim 3{\cdot}10^6 K$) and a hard ($\sim 10^7 K$) component (Cassinelli and Swank, 1983, cf. also Chen and White, 1991). The original picture of a *base* corona can be excluded (cf. Baade and Lucy, 1987, and references therein), and it is generally assumed that the emission must originate from well above the base, most probably from shocks embedded in the wind. The above temperatures then imply corresponding shock speeds (with respect to the underlying flow) of the order of 500 km/s.

With the succesfull launch of *ROSAT*, present efforts concentrate on detailed modelling of the observed spectra. Again for the case of ζPup, our results indicate the fluxes created in such shocks to agree well with the (PSPC = *P*osition *S*ensitive *P*roportional *C*outer-) observations, *if the background opacities from our present wind model* (cf. §2) are taken into account (Kudritzki and Hillier, 1992; Hillier et al., 1993). Unfortunately, as the observed soft X-rays are emitted at very large distances from the star (up to 1000 R_*) and the hard component gives an only weak constraint for the minimum radius of emission ($R_{\rm Min} \lesssim 2R_*$), this analysis can provide almost no information - up to the required shock speeds - about the structure in the lower wind part.

Black troughs in P-Cygni profiles of resonance lines. As was already

mentioned in §2.2.2, theoretical UV P-Cygni profiles differ significantly from the observed line shape if a stationary, monotonic outflow is assumed and the intrinsic line profile is purely Doppler-broadened by the ionic *thermal* motion, without any additional "turbulent" velocity. As an example, we show in Fig. 8 the NV doublet for ζPup, where the dashed and solid curves line give the synthetic profiles assuming respectively $v_{turb}= 0$ and $v_{turb}^{max} \approx 250 km/s$ It is evident that both the observed blackness and the decline to zero intensity (as well as the rise to the emission peak) are only reproduced by the model with strong *supersonic* turbulence. Of course, such introduction of strong turbulence here is entirely *ad hoc*.

On the other hand, Lucy (1982, 1983) noted that this observed degree of blackness can be produced by a *multiply non-monotonic* flow. This process will be discussed in more detail in §3.3.1

Discrete absorption components indicate most directly a structure and temporal variability in the winds. These relatively narrow features are superimposed on the blue absorption parts of P-Cygni lines. They typically form at half v_∞ and then narrow and shift to higher velocities over several days (Prinja and Howarth, 1988; Henrichs, 1988 and references therein). Their recurrence and acceleration time seems to be correlated with the stellar rotational period (Prinja, 1988). As an example, Fig. 9 shows the temporal evolution (time running up) of such a component in the SiIV spectrum of 68 Cyg (O7.5 III:n ((f))). In the upper panel, 29 spectra covering three and a half day are superimposed, whereas the lower panel gives a grey-scale rendition of intensity. The evolution of the DAC (present in both doublet components) as described above is obvious. The reader may also note that the *emission part* of the P-Cygni profiles remains rather stable.

Profile variability is evident both in UV and optical spectra. Fig. 10 shows the "blue-edge variability" present in UV P-Cygni profiles for the example of the CIV resonance line of λCep (O6I(n)fp) as an overlay (23 spectra covering 2.5 days) and grey scale rendition; Fig. 11 shows the variability of the HeII 4686 ($\dot{M}$ indicator!) line from 43 spectra covering two days ($\Delta t \approx 15...30$ min).

The obvious question is now, whether all these features (inclusive those mentioned briefly in §1) are, as is often argued, only the manifestation of some "second order effects" acting on an essentially smooth flow, or, more adequately, represent the "tip of an iceberg", pointing towards a considerably different physical description of the winds. In order to answer this question, the assumption of stationarity has to be abandoned and the time-dependence explicitly taken into account!

3.2 Basic Features of Time-Dependent Simulations

(In this section, we will recapitulate only some important results with no intention of completeness; for recent reviews, cf. Owocki, 1992, and Castor, 1991.)

One of the most important results from formal stability analysis of line-driven flows (cf. MacGregor et al., 1979; Carlberg, 1980; Abbott, 1980; Lucy, 1984; Owocki and Rybicki, 1984 (OR), 1985) is the recognition that the line acceleration is highly unstable against velocity disturbances, at least if the disturbance is optically *thin*, meaning that one can ignore any change in optical depth.(Optically thick disturbances lead to stable situations, as here a phase shift of $\sim 90°$ between disturbance

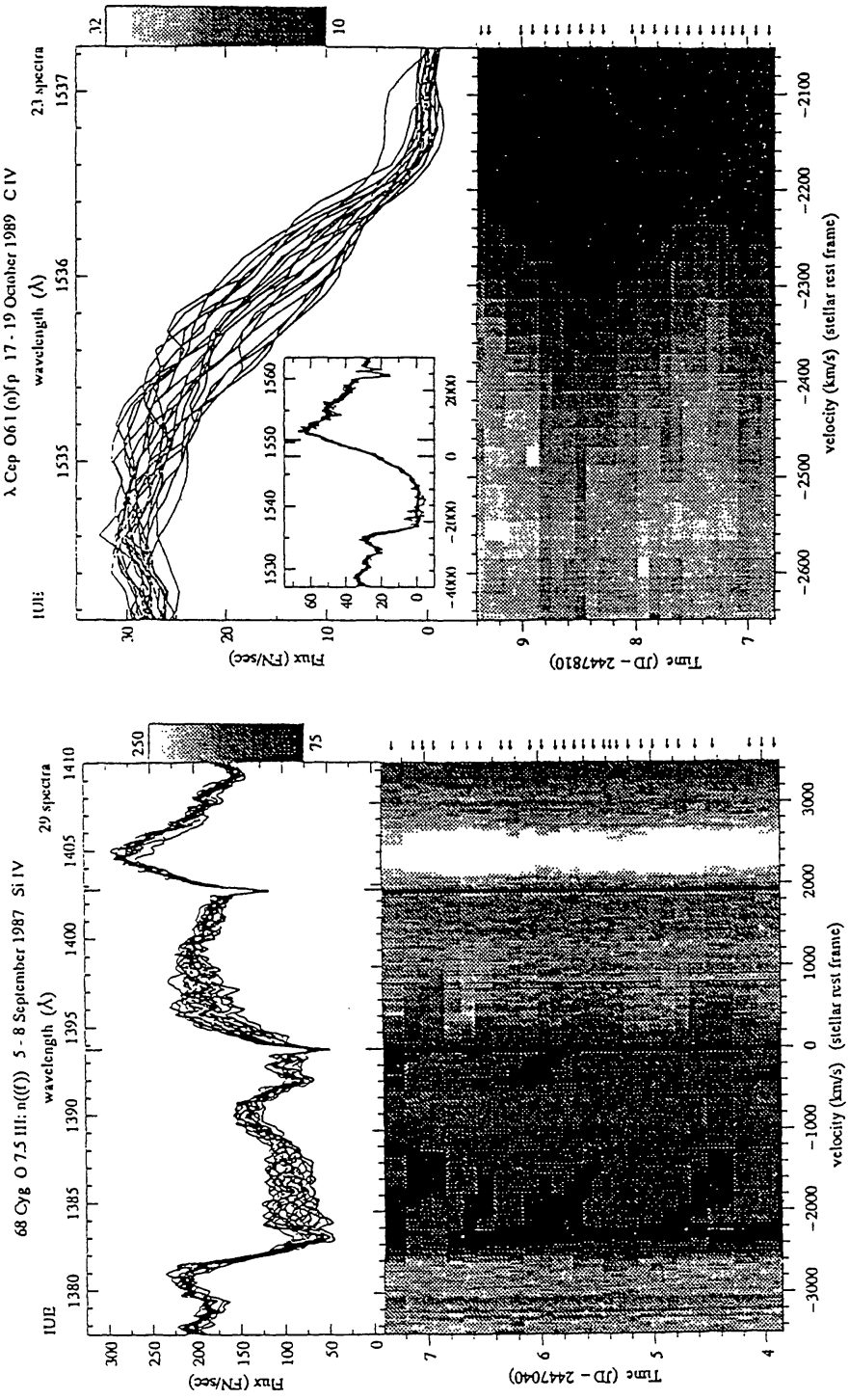

Figure 9: (left) Temporal evolution of DAC's (time running up, for details see text). (From Henrichs, 1991.)

Figure 10: (right) Variable blue edge in CIV P-Cygni profile (time running up, for details see text). (From Henrichs, 1991.)

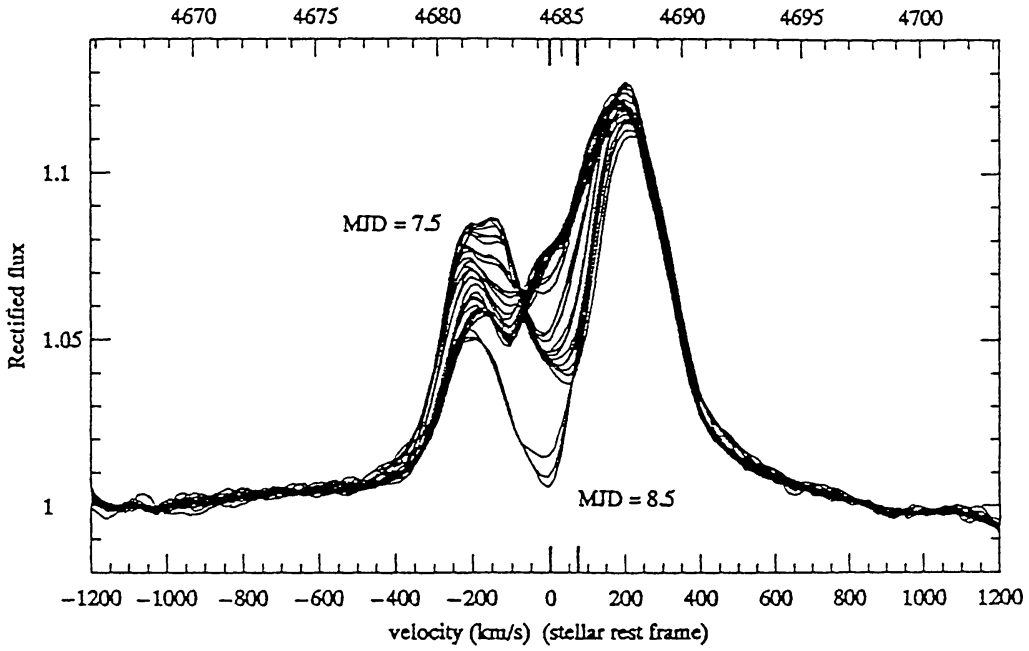

Figure 11: Variability in HeII 4686 ($\Delta t \approx 15...30$ Min). (From Henrichs, 1991.)

and reacting line-force is created, so that no net-work is done (Abbott, 1980); the "unification" of both limiting situations was achieved by OR leading to the so-called "bridging law".)

By neglecting the diffuse radiation field caused by reemission processes (see below), this effect is easily understood:

In analogy to the zeroth order process which is responible for the line-force (cf. §2.1), an arbitrary (positive) velocity disturbance δv will primarily shift the profile with respect to the continuum, so that additional momentum from *unprocessed* photospheric photons is transferred to the ions. Hence, the line force is increased, which leads to a further increase of velocity and so on. For a typical scale height $\rho/(d\rho/dr)$, the cumulative growth of this unstable process is of the order $2v(r)/v_{th}$, where v_{th} is the thermal speed of the ion (cf. OR). Thus, the growth can approach enormous values (up to ~ 100) in these highly supersonic winds.

In addition, the flow is most unstable against *inward propagating* waves, which, as they steepen due to non-linear effects, finally form strong *reverse* shocks. These reverse shocks are the most prominent features associated with the line-force instability. They differ from the more familiar forward shocks by the fact that (in the *stellar* frame)

$$v_{pre} > v_{post} > v_{shock}^{reverse}$$

These shocks thus travel backwards in the comoving frame (but outwards in the stellar frame) with the pre-shock side directed towards the star. In this case, the *density is high where the velocity is low* (cf. Fig. 12), in contrast to the forward shock situation where the density is large at large velocities.

Although it became evident that inclusion of just the *"direct"* force (resulting from absorption-processes only) leads to an *absolute* instability (Owocki and Rybicki, 1986), there exist at least two processes which can partly stabilize the flow.

First, the *"line drag"* resulting from scattered photons inside the interaction zone (Lucy, 1984) leads to a perturbation in the *diffuse* radiation force which acts

to oppose to the velocity-disturbance: $\delta g^{\rm diff} \sim -\delta v$ and thus stabilizes the process. An instructive discussion of this effect is given by Owocki (1992); it is presently approximated by the so-called "smooth source function" approach (SSF, Owocki, 1991).

Second, the *thermalization* of lines can also introduce a stabilization (cf. Feldmeier and Owocki, in prep.), whereas in the present approach only scattering events are accounted for.

Both effects, however, are significant only in regions with $v \leq v_{sonic}$, whereas the supersonic flow remains rather unstable.

Basic Assumptions for (Present) Hydrodynamical Calculations

1-D formulation: In order to investigate the principle processes, the present 1-D treatment is sufficient, as the *horizontal* instability of the line-force is strongly damped by the line-drag effect (cf. Rybicki, Owocki and Castor, 1990). It should be emphasized, however, that the description of the wind structure in terms of *shells* extending around the star is entirely an artefact of the restriction to 1-D spherical symmetry. In an actual 3-D wind, such shells are likely to be broken up in "clumps" with a limited angular extent. However, as follows from the presence of the DAC's, a significant fraction of the solid angle subtended by the stellar disk is covered by absorbing material at comparable velocities, which may place a lower limit on the *lateral* scale of the structure.

Isothermality: Another severe restriction is the isothermal approach, which assumes that the *cooling length is small compared with competing length scales*. This is certainly *not justified* for low $\dot{M}$ and large radii, where the cooling length can become comparable to the stellar radius. (For scaling relations, see Krolik and Raymond, 1985; Castor, 1987; Chen and White, 1991; Hillier et al., 1993.) As an example, for a $\dot{M} \approx 3 \cdot 10^{-6} M_{\odot}/yr$ and $R_* = 20 R_{\odot}$, the cooling length in our structured model (see below) is quite small compared to the extension of the shells for $r \lesssim 4...5 R_*$, whereas a statement concerning the structure in the outer wind part is not possible at present (cf.§3.3.2).

In order to solve this problem, as well as to investigate the X-ray (+ EUV, cf §2.1) emission of the shocked plasma in the cooling zones, the energy transfer has to be incorporated in the present description. The solution of this problem is well under way; for first results see Cooper and Owocki (1991) and the poster-paper presented by Feldmeier and Puls at this conference.

A Radiation-Hydrodynamics Model

The stellar wind model used here is computed using the radiation-hydrodynamics code described in Owocki, Castor and Rybicki (OCR, 1988), modified for the diffuse radiation force (SSF-formalism; Owocki, 1991), where the assumptions discussed above have been applied. The adopted stellar wind parameters are those for a generic O-type supergiant, T_{eff}= 50,000 K, $R_* = 20 R_{\odot}$ and $M_* = 50 M_{\odot}$. For numerical details, see Puls and Owocki (1993).

The initial condition is taken from a corresponding "mCAK" stationary model, obtained with a CAK/Sobolev treatment of the line-force, modified to take proper

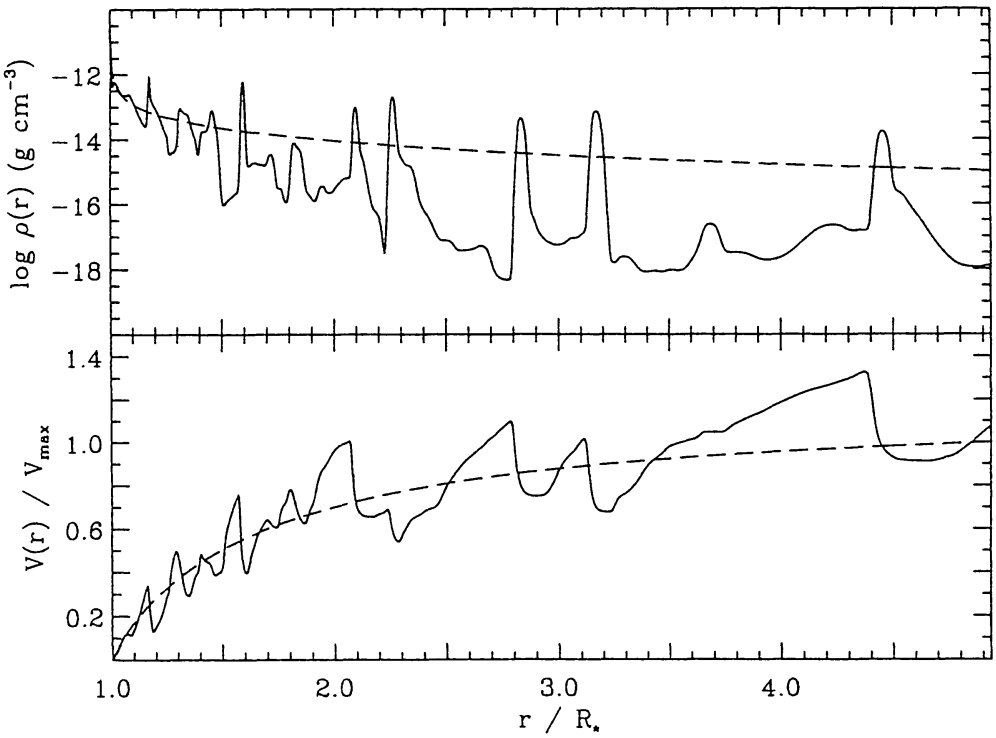

Figure 12: Density and velocity vs. radius in a dynamical structured wind at a fixed snapshot (for details, see text). (From Puls and Owocki, 1993.)

account of the finite stellar disk (Pauldrach et al. 1986). The wind parameters are $\dot{M} = 2.4 \cdot 10^{-6} M_{\odot}/yr$ and $v_{\infty}^{\rm mCak} \approx 2,000 km/s$.

The boundary conditions are as described in OCR, and allow for the introduction of a base perturbation at the lower boundary in the form of an upward-propagating sound wave. For simplicity, this perturbation is assumed here to be sinusoidal with period 10,000 sec. To induce a substantial wind structure that will challenge and test our spectrum synthesis methods, we use a quite large perturbation amplitude of $\delta\rho/\rho = \delta v/a = 0.25$, where ρ, v, and a are the density, velocity, and sound speed. This large amplitude compensates for the line-drag reduction of the instability and thus leads to nonlinear structure relatively close to the wind base ($r \gtrsim 1.1 R_*$).

Fig. 12 compares the radial variation of density and velocity in the mCAK initial condition (dashed curves) with a snapshot of the structured wind at a fixed, arbitrary time $t = 60,000$ sec later (solid curves). Note the presence of numerous strong, *reverse* shocks in which high-speed, very-low-density flow is decelerated as it impacts into relatively slow material that has been compressed into narrow, dense shells. The visual dominance of the high-speed rarefactions in this plot is somewhat misleading, since only very little wind material is accelerated to these high speeds.

Finally, because the pre-shock material is extremely rarefied, only a small fraction of the gas $\lesssim 10^{-3}$ is actually shocked which implies that a similar small fraction of the total kinetic energy $\sim \dot{M} v_{\infty}^2/2 \approx 10^{-3} L_{Bol}$ goes into shock heating, which thus may explain qualitatively the observed scaling law $L_x \sim 10^{-7} L_{Bol}$. Note, however, that our present analysis of ROSAT observations imply the *observed* X-ray luminosity to be considerably smaller than the total emitted one (percentage level, cf. Hillier et al., 1993).

3.3 Spectrum Synthesis in Time-Dependent Simulations

As was pointed out in the introduction, " ... one of the most urgent needs is to develop methods to compare more closely predictions from the theoretical simulations with available observational diagnostics, and thereby guide and test the further theoretical development..." (from Owocki, 1990, AG-conference in Berlin on "Accretion and Winds").

This task is the aim of a present collaboration of the Munich and Bartol wind groups. In order to start this project, we have at first to question in how far the transfer in stationary and time-dependent models actually differ.

Roughly, two different processes have to be distinguished:

1. Resonance line transfer

– Transfer effects are dominating only in *distinct* regions ($\rightarrow$ shells/clumps), as the intershell medium is extremely rarefied.

– In these regions, the density is larger than in the corresponding stationary models, and the velocity gradient can be *negative* (cf. Fig. 12).

– The velocity field is *non-monotonic*, hence we have to account for the *radiative coupling* of different locations with a zero difference of projected velocity.

2. Density-squared dependent opacities (H_α, IR, Radio)

– Due to the clumpiness of the structure, the (both spatial and temporal) average of $< \rho^2 >$ is larger than $< \rho >^2$, so that an enhanced emission is to be expected (cf. Abbott et al., 1981; Lamers and Waters, 1984a).

3.3.1 Resonance Line Formation

(For a detailed discussion, see Puls and Owocki, 1993)

Our focus here will be to examine line-diagnostics for which the opacity scales roughly linearly with density (e.g. UV resonance lines). As was pointed out above, the simulation models for these calculations were purposely chosen to contain substantial structure, in order both to challenge and test the methods and to obtain clear effects. They thus define an extreme, rather than a "best-fit" structure model. In addition to the question of the difference with respect to transfer in stationary models, we want to clarify the general requirements for such models to reproduce commonly observed nonstationary features, as the blue-edge variability and the black troughs of saturated lines. (Unsaturated lines and DAC's are not considered here, but cf. Puls and Owocki.) Once reliable techniques for synthesizing observational signatures are at hand, we eventually intend to make more detailed comparisons with observational data, in order to refine these models, and hopefully thereby obtain a clearer picture of the structure of such stellar winds.

The major challenge in synthesizing P-Cygni lines is to determine a consistent source-function that accounts for all radiative couplings, because the shape of the profile for saturated lines is determined by the reemission process. In the following, for reasons of simplicity, we consider only the formation of a resonance singlet and assume the line to be pure scattering. This last assumption allows us to check the precision of our solution, since in this case the equivalent width of the profile (corrected for backscattering onto the stellar core) has to be zero!

Creation of a Black Trough by a *Multiple Non-Monotonic Flow*

(cf. Lucy, 1982 and 1983)

In order to understand better the results of the next section, we want to review briefly how a multiply non-monotonic flow can establish the formation of a black trough. In analogy to Lucy's (1982a) *empirical* shock model we assume here that the number of shocks per Δr is large, so that the number of radiatively coupled resonance zones N is high. In this so-called "scattering complex" then, all source functions $S_i(\mu v_i = \mu v_1)$, i = 1,N are radiatively coupled, if N_1 denotes the first encountered resoncance zone irradiated by unprocessed photospheric continuum.

In the limit of large N, plane-parallel geometry (which is justified for large N) and an optically thick scattering line, it is relatively easy to show (by means of Sobolev theory, but cf. also the derivation by Lucy, 1982) that

$$\begin{aligned} S_1 &\rightarrow \frac{2N}{N+1} S_0^{\rm local} &\rightarrow 2S_0^{\rm local} \\ S_N &\rightarrow \frac{2}{N+1} S_0^{\rm local} &\rightarrow 0 \end{aligned}$$

if $S_0^{\rm local}$ denotes the purely *local* source function at the begin of the scattering complex which would be present in the *absence* of any non-local coupling.

Hence, such a complex (for large N) can be treated as one *back-scattering* zone. Note, however, that the local source function $S_0^{\rm local}$ can be different from the *stationary* one due to the presence of the large velocity gradients required to establish such a complex.

The resulting P-Cygni profile has then the following stucture: The blue side is completely (plane-parallel geometry) black, as the observer sees here the *backside* of the scattering complexes. Hence, there are no photons which are scattered into the observer's direction, so that the absorption trough is not refilled. On the other hand, in the red side we see the receding part of the wind and hence the front side of the complexes, so that here the profile exhibits roughly double the continuum level.

Radiative Coupling in Shell Models

From Fig. 12, it is obvious that our hydrodynamical model shows (in addition to the reverse shock structure) a number of differences to the heuristic, nonmonotonic velocity model which influences the quality and strength of the non-local coupling.

- The number of radiatively coupled points is *smaller*, as the number of shells covering the same range in velocity is low (N=2..3).
- In the lower wind region, the velocities are unique, so that no coupling occurs.
- Transfer effects play a rôle primarily inside the shells, which cover an only small spatial extent of the wind, so that the effective scattering *area* is also small.
- Due to sphericity and the radial separation of the shells, the coupling covers only a small part of the complete solid angle.

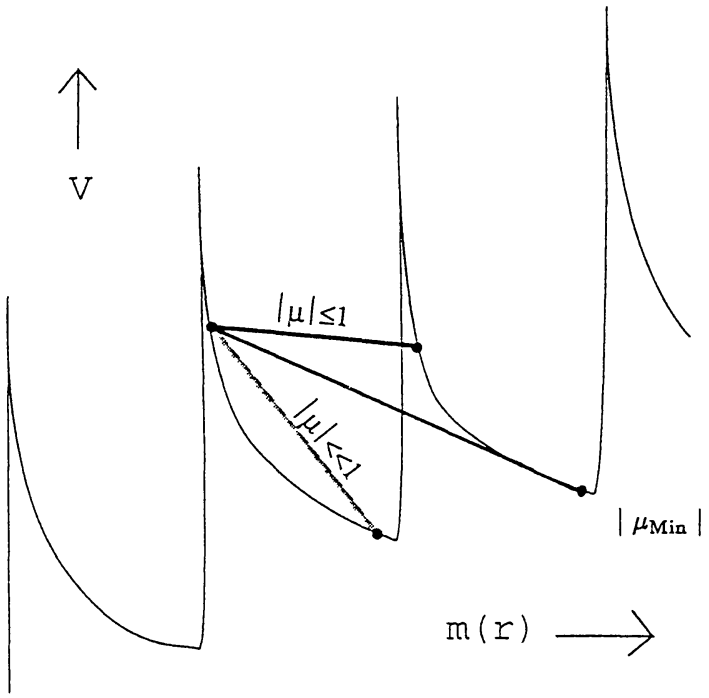

Figure 13: Schematic of the mass variation of velocity, showing intrashell couplings at oblique directions $|\mu| \ll 1$ and intershell couplings at nearly radial directions $|\mu| \lesssim 1$. (From Puls and Owocki, 1993.)

Fig. 13 illustrates the situation for two successive shells, now plotted as function of a *mass* coordinate, defined here as $m(r) \equiv 4\pi \int \rho(r') r'^2 dr'$.

Note that the high-speed rarefactions now appear as mere spikes, emphasizing that such structures really involve very little material. From this figure, it is obvious that two different kinds of coupling may occur:

- *intrashell* coupling for angles $\mu'_{\rm Max} < \mu \lesssim 0$
- *intershell* coupling for angles $1 \leq \mu \leq \mu_{\rm Min}$, which in the present case is dominating, where

$$\mu_{\rm Min} = \left(\frac{1}{1 + \frac{\Delta v}{v} / \frac{\Delta r}{r}} \right)^{\frac{1}{2}},$$

(cf. Puls and Owocki), Δv the range of overlapping velocities and Δr the separation of the shells (Fig. 13).

From the definition of $\mu_{\rm Min}$ it is clear that an effective coupling which occurs for $\mu_{\rm Min} \to 0$ requires either a large velocity amplitude or a small separation of the shells. As both requirements are not met in our present model (the average value of $< \mu_{\rm Min} > \approx 0.85$), we cannot expect dramatic intershell effects.

Fig. 14 now shows the profile for a strong line resulting from the consistent source function allowing for all non-local couplings (fully drawn) based on the hydrodynamical snapshot Fig. 12, in comparison to the profile (same line-strength) calculated for the smooth flow with $v_{turb} \equiv 0$ (dashed, for computational details, see Puls and Owocki). Both profiles have, as theoretically required, an equivalent width of zero

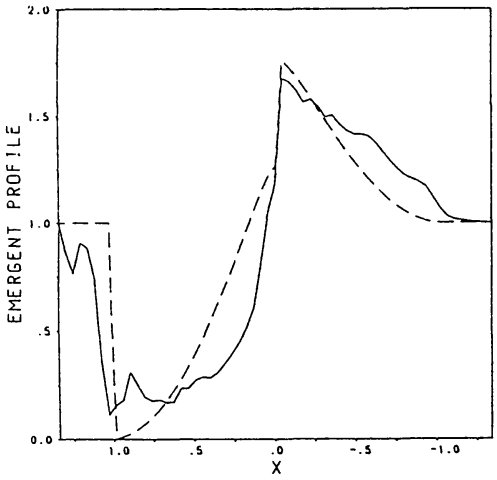

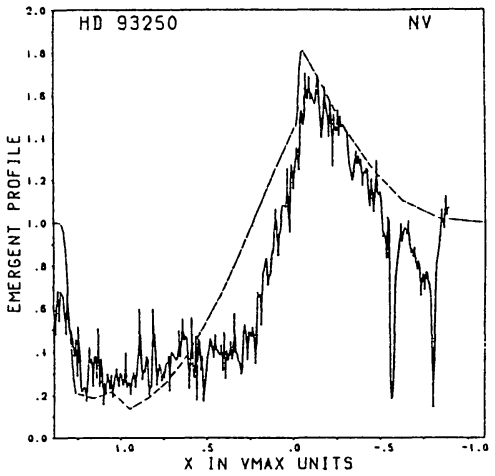

Figure 14: (left) Emergent profiles vs.dimensionless frequency $x = (\nu/\nu_o - 1)c/v_{\rm mCAK}(R_{max})$ for a strong line and the structure-wind snapshot of Fig. 12 (fully drawn) and the smooth model (dashed). (From Puls and Owocki, 1993.)

Figure 15: (right) SEI-fit to the NV doublet of HD 93250 (O3V). In this fit, an artificial, velocity-dependent micro-turbulence was adopted, with $v_t(r) \approx 0.1v(r)$ and $v_t^{\rm min} \approx 60km/s$. (From S. Haser, p.c.)

after correction for back-scattering, indicating the high accuracy of the algorithm. For the same line-strength, we show in Fig. 16 the *time series* of the profiles emerging from the structured model at ten 1000-sec intervals starting from the snapshot time.

The good news: From Fig. 14, we see that a broad trough is created, which on the bluest side is due to the high velocity components and for low velocities stems primarily from a reduction of the effective scattering area (see above). This reduced emission now is in the right direction for reproducing observed profile shapes, which often show just this "extended region of absorption" at low velocities (cf. Groenewegen and Lamers, 1989, Fig. 2) As a typical example we show in Fig. 15 the NV ($\lambda\lambda$ 1238,1242) doublet of HD 93250 (O3V). The discussed feature (+ the extended, gradual blue wing) can be reproduced by our model *without* any adopted *"micro"*-turbulence, which in typical line-fits (e.g. Hamann,1981; Puls, 1987; Groenewegen and Lamers, 1989) results in values of the order of 10% of v_∞. Worse, a fit of the "extended absorption" with stationary models would require unreasonably/unphysically high turbulence velocities *near the photosphere* of the order of *several times* the sound speed, i.e. supersonic turbulence inside the photosphere, which is in strong contrast to photospheric NLTE analyses and would also shift the emission peak to the red, in contrast to observations. Using alternatively a reasonable (i.e. velocity dependent) turbulence cannot explain this extended absorption (cf. Fig. 15).

From the temporal evolution of the strong line (Fig. 16), we find both the emission and the inner absorption part to show only weak evidence of structure and variability, in agreement with observations. (Note, that these snapshots are additionally averaged because of a finite exposure time.) However, there are quite significant variations at the *blue edge*, which often extends substantially beyond the

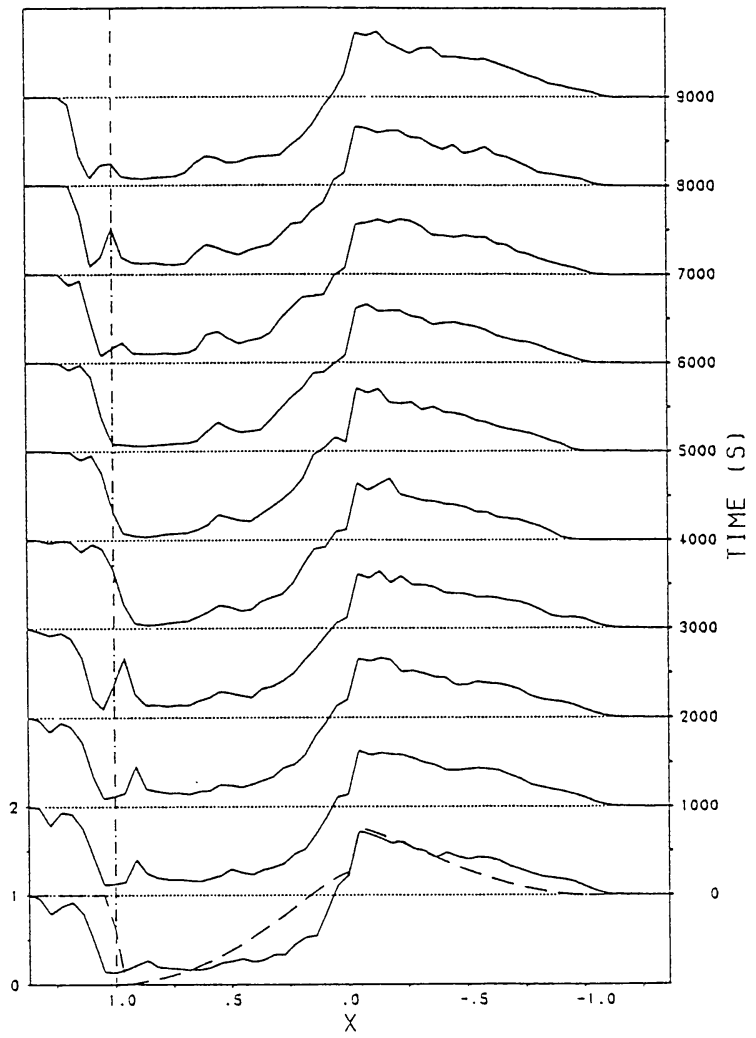

Figure 16: Time series of emergent flux profiles for the structured wind and a strong line at ten 1000-second intervals beginning at the snapshot Fig. 12. (From Puls and Owocki, 1993.)

edge for the stationary model.

In contrast to the very sharp edge of the stationary case, the blue edge in the structured model also tends to be quite gradual, implying that there is a range of frequencies over which the wind is only marginally optically thick. The material responsible for this blue-edge absorption must have flow velocities that extend well above the steady-wind terminal speed, but, since the absorption is unsaturated despite the high line-strength, it must have only a low to moderate density. Inspection of plots of structured model velocity and density vs. radius (e.g. Fig. 12) show that such high speed regions are, in fact, often quite low-lying ($r \approx 2-3R_*$). This is thus in quite marked contrast with the usual association of the blue edge in stationary models with the wind's *terminal* speed.

The bad news: As the blue part in these strong lines is typically filled in with a substantial emission, the P-Cygni profiles for these structured models do *not* repro-

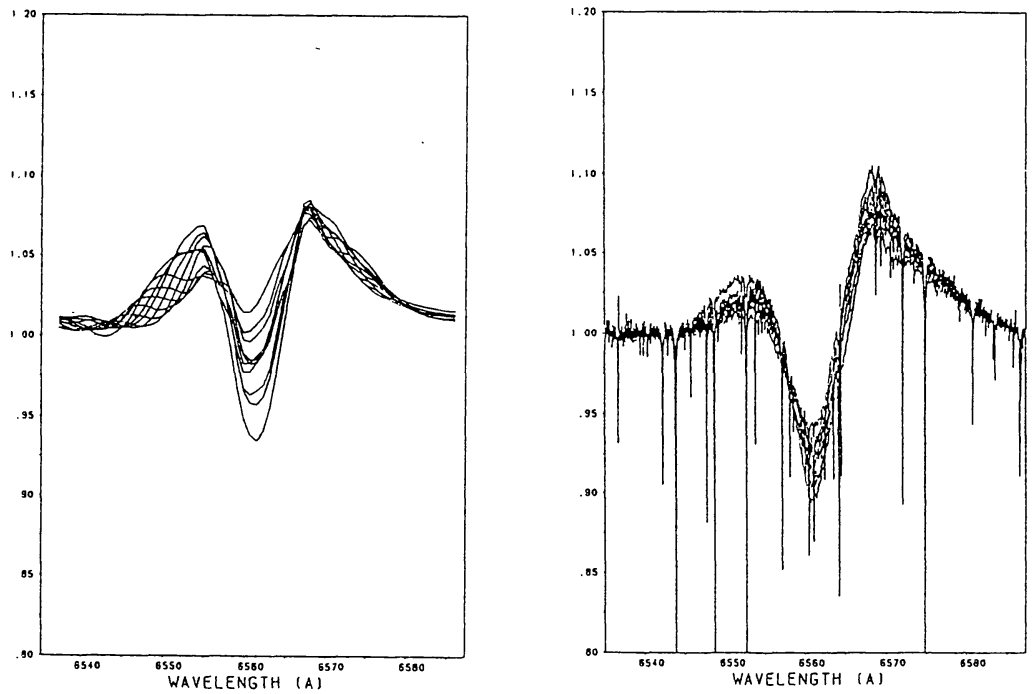

Figure 17: (a) Overlay of emergent H_α-profiles for the structured wind at ten 1000-second intervals beginning at the snapshot Fig. 12. (b) Sequence of H_α-observations of ζPup (for details, see text, observations by D. Baade, p.c.).

duce very well the black troughs characterically observed for strong resonance lines. Because of the above reasons and the relatively low outer boundary $R_{max} \approx 5R_*$ (isothermal approach!) in the present model, the possible number of resonances is simply not sufficient to suppress adequately the forward scattered radiation that fills in absorption trough.

In this regard, it is important to emphasize that the particular dynamical parameters chosen here were not aimed specifically at producing such black troughs. Thus, determining whether such dynamical, structured-wind models might, in principle, produce black troughs must await a future, more systematic and extensive parameter study.

3.3.2 Density Squared Dependent Opacities

This section states some preliminary results of a present collaboration (cf. also Owocki, 1992), for details see Puls, Najarro and Owocki (1993, in prep. for *Astron. Astrophys.*).

The $\dot{M}$–Indicator H_α

By simulating the formation of H_α (incl. HeII blend) in our structured wind model and comparing this to observations, we are able to test the clumping in the lower wind part, because these lines are typically formed in a region with $v_{\rm stat.} \lesssim 0.5 v_\infty$. Fig. 17a compares a timeseries of such synthetic profiles with a time series of observations of ζPup (Fig. 17b). For the simulations, we adopted NLTE-departure coefficients in analogy to the results from unified models (cf. Gabler et al., 1989)

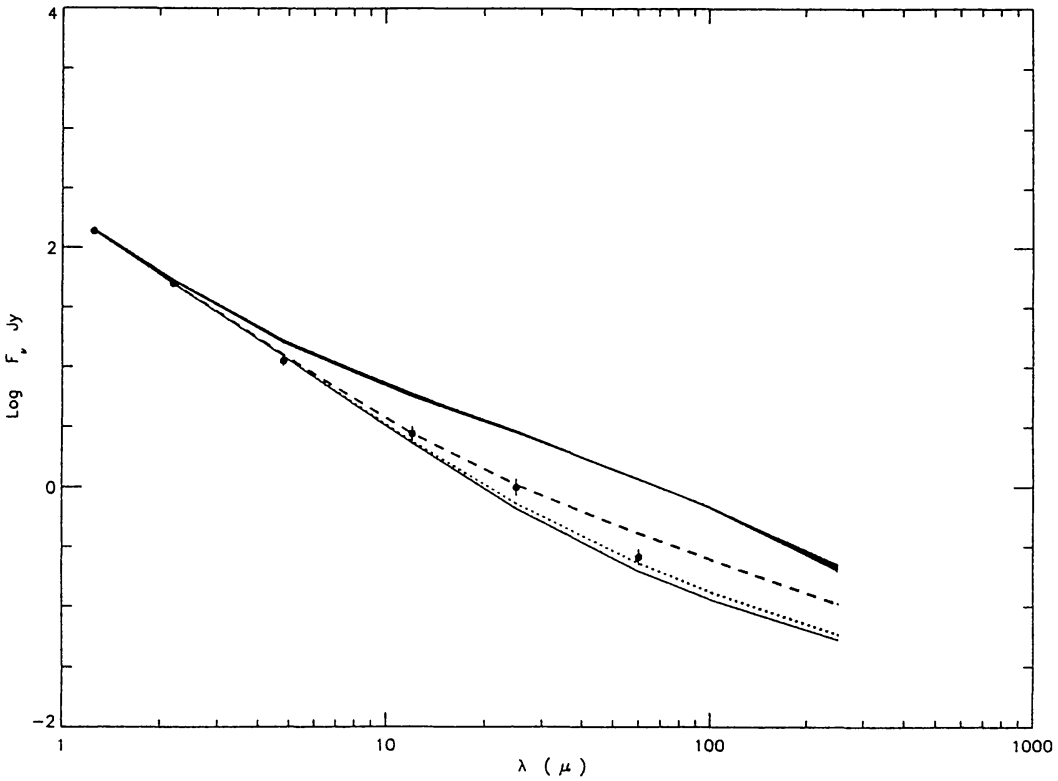

Figure 18: Emergent IR-flux of different models (see. text) vs. observations (beyond 10 μ by Lamers et al., 1984 (IRAS), below by Tanzi et al., 1984, (p.c. to H. Lamers.)).

(however differing not drastically from unity). The observations were obtained by D. Baade (p.c.) with the ESO 1.4m telescope and the Coudé spectrograph ($\sim$ 3 observations per night resulting in 33 exposures in total). From a comparison, we find a good agreement in both the shape *and* the equivalent width. Note, that stationary models need roughly a factor 2 more $\dot{M}$ to obtain the same equivalent width, which is a result of the presence/absence of clumping.

IR-Formation

The analysis of the IR-formation allows us to investigate the clumping in the intermediate part of the wind ($2...10 R_*$). Provided the *actual* wind has a structure comparable to our model, i.e. provided that it consists of dense clumps and an almost *void* medium in between, it can be shown (cf. Abott et al, 1981; Lamers and Waters, 1984a) that the $\dot{M}$ *deduced* assuming a stationary flow will overstimate the actual $\dot{M}$ by a "clumping factor" $cf = (\rho^+/\rho_{\rm stat.})^{0.5}$, if ρ^+ denotes the typical density inside the clumps. In Fig. 18, we compare the synthetic IR-flux (fully drawn, based now on a model with $\dot{M} = 3 \cdot 10^{-6} M_\odot/yr$) both with the observations (dots) and the flux arising from stationary models (fully drawn, lowest curve). It is obvious that our clumped model produces much too much flux, which is primarily due to the large average $< cf > \approx 3.6$. However, as indicated by the dashed curve, a model with the same clumping but considerably lower $\dot{M} \approx 1 \cdot 10^{-6} M_\odot/yr$ is almost able to reproduce the observations.

Radio-Formation

One of the most important topics is the formation of the radio emission, as this occurs in the most outer wind part ($r \gtrsim 50R_*$ in case of ζPup) and is almost unbiased by any assumption up to the strength of the clumping (Additionally, as shown by Hillier et al. (1993), this is just the region where the observed soft X-rays are emitted.). However, because of limitations in both computing time and in the treatment of energy balance, our hydrodynamical simulations have not yet been extended to this region.

In this context, one has to note that from the diagonistics of *stationary* models all $\dot{M}$'s derived by the above three methods agree (at least for thermal emitters), i.e.

$$\dot{M}_{\mathrm{H}\alpha} \approx \dot{M}_{\mathrm{IR}} \approx \dot{M}_{\mathrm{Radio}} \,|_{\mathrm{stat.}}$$

(cf. Gabler et al., 1989, Kudritzki et al., 1992). This equality can be reached in principle also for clumped models, provided that the clumping is roughly constant throughout the wind. In this case then, the actual $\dot{M}$ would be smaller than the presently derived one.

On the other hand, if theoretical investigations showed that a clumping is not possible in the outer wind part, then the above equality would imply that the inner wind could also not be very clumped.

4 Conclusions and Future Work

The investigation of resonance line formation in dynamical, structured models of radiatively driven winds shows that the formation is completely different from the formation in stationary models. The calculated profiles look "reasonable" and may explain a number of observational features. A future systematic investigation and parameter study should enable us to provide useful constraints on the geometry and actual structure of hot star stellar winds, at least in the inner, roughly isothermal regions. One of the next steps should incorporate the question of black trough formation, which most probable will require a 2-D treatment in order to simulate a more realistic clump instead of a shell structure.

The simulation of processes involving density squared opacities will become a useful tool to investigate the clumping as function of radius (consider also the sub-mm observations, cf. Leitherer and Robert, 1991), especially in the outer wind parts. However, before this aim can be accomplished, a number of different problems have to be solved. Most important is the incorporation of the energy equation and the consistent treatment of the line force as function of temperature. After results become available, the structure at large radii and the X-ray synthesis should give further insights into the realism of these models.

Not discussed so far is the influence of the different structure on the occupation numbers. Here, the increased density and the hot radiation field emitted by the shocks are competing processes, which have to be considered by detailed NLTE-calculations.

Finally, we have to look for additional diagnostic tools for a further, hopefully unique discrimination between stationary and non-stationary models. One of this tools may be the investigation of IR-lines, which will become possible with the upcoming ISO-mission.

Acknowledgements. Many thanks to Dr. Dietrich Baade for providing us his H_α–observations of ζPup. This project was partly supported by DFG grants Pu 117/1-1, Pa 477/1-1, 418 SPA - 112/1/90 (Munich group) and by NSF grant AST 91-15136 and NASA grants NAGW-2624, NAG5-1657 (S.P.O.). J. Puls gratefully acknowledges a travel grant by the Max-Planck-Institut für Astrophysik. Many of the computations were carried out at the Leibniz Rechenzentrum, Munich and using an allocation of supercomputer time from the San Diego Supercomputer Center. We thank A. Feldmeier and A. Fullerton for helpful discussions and comments.

References

Abbott, D. C.: 1980, *Astrophys. J.* **242**, 1183
Abbott, D. C., Bieging, J. H., Churchwell, E.: 1981, *Astrophys. J.* **250**, 645
Abbott, D. C.: 1982, *Astrophys. J.* **259**, 282
Abbott, D. C.: 1982a, *Astrophys. J.* **263**, 723
Abbott, D. C., Bieging, J. H., Churchwell, E.: 1984, *Astrophys. J.* **280**, 671
Abbott, D. C., Hummer, D. G.: 1985, *Astrophys. J.* **294**, 286
Baade, D., Lucy, L. B.: 1987, *Astron. Astrophys.* **178**, 213
Becker, S. R., Butler, K.: 1992, *Astron. Astrophys.* , in press
Carlberg, R. G.: 1980, *Astrophys. J.* **241**, 1131
Cassinelli, J. P., Olson, G.L.: 1979, *Astron. Astrophys.* **229**, 304
Cassinelli, J. P., Swank, J. H.: 1983, *Astrophys. J.* **271**, 681
Castor, J. I.: 1970, *Monthly Notices Roy. Astron. Soc.* **149**, 111
Castor, J. I., Abbott, D. C., Klein, R.: 1975, *Astrophys. J.* **195**, 157
Castor, J. I., Abbott, D. C., Klein, R.: 1976, in *Physique des Mouvements dans les Atmosphères Stellaires*, eds. R. Cayrel and M. Steinberg, Paris, CNRS, p. 363
Castor, J. I.: 1987, in *Instabilities in Luminous Early Type Stars*, eds. H.J.G.L.M. Lamers and C.W.H. de Loore (Reidel, Dordrecht), p. 159
Castor, J. I.: 1991, in *Stellar Atmospheres: Beyond Classical Models*, eds L. Crivellari, I. Hubeny and D. Hummer, (Kluwer, Dordrecht), p. 221
Chen, W., White, R. L.: 1991, *Astrophys. J.* **366**, 512
Chlebowski, T., Harnden, F. R.,Jr., Sciortione, S.: 1989, *Astrophys. J.* **341**, 427
Cooper, R. G., Owocki, S. P.: 1991, in *Nonisotropic and Variable Outflows from Stars*, eds. L. Drissen, C. Leitherer and A. Nota, (Astron. Soc. Pacific, San Francisco), p. 281
Drew, J. E.: 1990, *Astrophys. J.* **357**, 573
Ebbets, D.C.: 1982, *Astrophys. J. Suppl. Ser.* **48**, 399
Eissner, W., Jones, M., Nussbaumer, H.: 1974, *Comput. Phys. Comm.* **8**, 270
Friend, D., Abbott, D. C.: 1986, *Astrophys. J.* **311**, 701
Gabler, R., Gabler, A., Kudritzki, R. P., Puls, J., Pauldrach, A.W.A.: 1989, *Astron. Astrophys.* **226**, 162
Gabler, A., Gabler R., Pauldrach, A. W. A., Puls, J., Kudritzki, R. P.: 1990, in: *"Properties of Hot Luminous Stars", Boulder-Munich Workshop, Astronomical Society of the Pacific Conference Series*, ed. C. Garmany, **7** , p. 218
Groenewegen, M. A. T., Lamers, H. J. G. L. M., Pauldrach, A. W. A.: 1989, *Astron. Astrophys.* **221**, 78
Groenewegen, M.A.T., Lamers, H.J.G.L.M.: 1989, *Astron. Astrophys. Suppl. Ser.* **79**, 359
Hamann, W. R.: 1981, *Astron. Astrophys.* **93**, 353

Harnden, F.R., Jr.: 1979, *Astrophys. J. (Letters)* **234**, L51
Henrichs, H. F.: 1988, in *O Stars and Wolf-Rayet Stars*, eds P. S. Conti and A. B. Underhill, NASA SP-497, p. 199
Henrichs, H. F.: 1991, in *ESO Conference and Workshop Proceedings* **36**, ed. D. Baade, p. 199
Herrero, A., Kudritzki, R. P., Vilchez, J. M., Kunze, D., Butler, K., Haser, S.: 1992, *Astron. Astrophys.* **261**, 209
Hillier, D. J.: 1991, *Astron. Astrophys.* **247**, 455
Hillier, D. J, Kudritzki, R. P., Pauldrach, A. W. A., Puls, J., Schmitt, J. H.: 1993, *Astron. Astrophys.* , submitted
Hummer, D.G., Rybicki, G. B.: 1985, *Astrophys. J.* **203**, 258
Krolik, J. H., Raymond, J. C.: 1985, *Astrophys. J.* **298**, 660
Kudritzki, R. P., Simon, K. P., Hamann, W. R.: 1983, *Astron. Astrophys.* **118**, 245
Kudritzki, R. P., Pauldrach, A. W. A., Puls, J.: 1987, *Astron. Astrophys.* **173**, 293
Kudritzki, R. P., Hummer, D. G.: 1990, *Annual Rev. Astron. Astrophys.* **28**, 303
Kudritzki, R. P., Gabler, R., Kunze, D., Pauldrach, A. W. A., Puls, J.: 1991, in *Proceedings of STSc - Starburst Galaxies* **5**, ed. C. Leitherer, p. 59
Kudritzki, R. P., Hummer, D. G., Pauldrach, A. W. A., Puls, J., Najarro , F., Imhoff, J.: 1992, *Astron. Astrophys.* **257**, 655
Kudritzki, R. P.: 1992, *Astron. Astrophys.* , in press
Kudritzki, R. P., Hillier D. J.: 1992, in *Proc. of G. S. Vaiana Memorial Symposium "Advances in Stellar and Solar Coronal Physics"*, eds. J. Linski and S. Serio, in press
Kudritzki, R. P., Lennon, D. J., Becker. S. R., Butler, K. Gabler, R., Haser, S., Hummer, D. G., Husfeld, D., Pauldrach, A. W. A., Puls, J., Voels, S., Walborn, N. R., Heap, S. R., Bohannan, B., Conti, P., Garmany, C. D., Baade, D.: 1993, *ESO-proceedings*, ed. P. Benvenuti, in press
Kurucz, R. L., Peytremann E.: 1975, *SAO Special Report* **362**
Lamers, H. J. G. L. M., Gathier, R., Snow, T. P.: 1982, *Astrophys. J.* **258**, 186
Lamers, H. J. G. L. M., Waters, L. B. F. M., Wesselius, P. R.: 1984, *Astron. Astrophys.* **134**, L17
Lamers, H. J. G. L. M., Waters, L. B. F. M.: 1984, *Astron. Astrophys.* **136**, 37
Lamers, H. J. G. L. M., Waters, L. B. F. M.: 1984a, *Astron. Astrophys.* **138**, 29
Lamers, H. J. G. L. M., Cerruti-Sola, M., Perinotto, M.: 1987, *Astrophys. J.* **314**, 726
Leitherer, C.: 1988, *Astrophys. J.* **326**, 356
Leitherer, C., Robert, C.: 1991, *Astrophys. J.* **377**, 624
Long, K. S., White, R. L.: 1980, *Astrophys. J.* **239**, L65
Lucy, L. B., Solomon, P.: 1970, *Astrophys. J.* **159**, 879
Lucy, L. B.: 1982, *Astrophys. J.* **255**, 278
Lucy, L. B.: 1982a, *Astrophys. J.* **255**, 286
Lucy, L. B.: 1983, *Astrophys. J.* **274**, 372
Lucy, L. B.: 1984, *Astrophys. J.* **284**, 351
MacGregor, K. B., Hartmann, L., Raymond, J. C.: 1979, *Astrophys. J.* **231**, 514
Maeder, A.: 1990, *Astron. Astrophys. Suppl. Ser.* **84**, 139
Nussbaumer, H., Storey, P. J.: 1978, *Astron. Astrophys.* **64**, 139
Olson, G. L.: 1982, *Astrophys. J.* **255**, 267

Owocki, S. P., Rybicki, G. B.: 1984, *Astrophys. J.* **284**, 337
Owocki, S. P., Rybicki, G. B.: 1985, *Astrophys. J.* **299**, 265
Owocki, S. P., Rybicki, G. B.: 1986, *Astrophys. J.* **309**, 127
Owocki, S. P., Castor, J. I., Rybicki, G. B.: 1988, *Astrophys. J.* **335**, 914
Owocki, S. P.: 1990, in *Reviews in Modern Astronomy* **3**, (Springer, Berlin), p. 98
Owocki, S. P.: 1991, in *Stellar Atmospheres: Beyond Classical Models*, eds. L. Crivellari, I. Hubeny and D. G. Hummer, (Kluwer, Dordrecht), p. 235
Owocki, S. P.: 1992, in *The Atmospheres of Early-Type Stars*, eds. U. Heber and C. S. Jeffery, (Springer, Berlin), p. 393
Panagia, N., Felli, M.: 1975, *Astron. Astrophys.* **39**, 1
Pauldrach, A., Puls, J., Kudritzki, R.P.: 1986, *Astron. Astrophys.* **164**, 86
Pauldrach, A.: 1987, *Astron. Astrophys.* **183**, 295
Pauldrach, A., Puls, J., Kudritzki, R. P., Méndez, R. H., Heap, S. R.: 1988, *Astron. Astrophys.* **207**, 123
Pauldrach, A. W. A., Kudritzki, R. P., Puls, J., Butler, K.: 1990, *Astron. Astrophys.* **228**, 125
Pauldrach, A. W. A., Puls, J.: 1990, *Astron. Astrophys.* **237**, 409
Pauldrach, A. W. A., Puls, J.: 1990a, in *Reviews in Modern Astronomy* **3**, (Springer, Berlin), p. 124
Pauldrach, A. W. A., Puls, J., Butler, K., Kudritzki, R. P., Hunsinger, J.: 1993, *Astron. Astrophys.* , in prep.
Prinja, R. K., Howarth, I. D.: 1986, *Astrophys. J. Suppl. Ser.* **61**, 357
Prinja, R. K.: 1988, *Monthly Notices Roy. Astron. Soc.* **231**, 21P
Prinja, R. K., Howarth, I. D.: 1988, *Monthly Notices Roy. Astron. Soc.* **233**, 123
Prinja, R. K., Barlow, M. J., Howarth, I. D.: 1990, *Astrophys. J.* **361**, 607
Prinja, R. K.: 1991, in *Nonisotropic and Variable Outflows from Stars*, eds. L. Drissen, C. Leitherer and A. Nota, (Astron. Soc. Pacific, San Francisco)
Puls, J.: 1987, *Astron. Astrophys.* **184**, 227
Puls, J., Hummer, D. G.: 1988, *Astron. Astrophys.* **191**, 87
Puls, J., Pauldrach, A. W. A.: 1990, in: *"Properties of Hot Luminous Stars", Boulder-Munich Workshop, Astronomical Society of the Pacific Conference Series*, ed. C. Garmany, **7** , p. 203
Puls, J., Owocki, S. P.: 1993, *Astron. Astrophys.* , submitted
Rybicki, G. B., Owocki, S. P., Castor, J. I.: 1990, *Astrophys. J.* **349**, 274
Scuderi, S., Bonanno, G., Di Benedetto, R., Spadaro, D., Panagia, N.: 1992, *Astrophys. J.* **392**, 201
Seaton, M. J.: 1987, *J. Phys. B: Atom. Molec. Phys.* **20**, 6363
Sellmaier, F., Puls, J., Kudritzki, R. P., Gabler, A., Gabler, R., Voels, S. A.: 1993, *Astron. Astrophys.* , submitted
Seward, F. D. *et al.*: 1979, *Astrophys. J. (Letters)* **234**, L55
Sobolev, V. V.: 1957, *Sov. Astron. Astrophys. J.* **1**, 678
Springmann, U. W. E., Pauldrach, A. W. A.: 1992, *Astron. Astrophys.* **262**, 515
Voels, S.A., Bohannan, B., Abbott, D. C., Hummer, D. G.: 1989, *Astrophys. J.* **340**, 1073
Walborn, N. R., Panek, R. J.: 1985, *Astrophys. J.* **291**, 806
Wright, A. E., Barlow, M. J.: 1975, *Monthly Notices Roy. Astron. Soc.* **170**, 41